Geol Rundsch (1994) 83: 624–641

J.-L. Lenoir · D. Küster · J.-P. Liégeois · A. Utke
A. Haider · G. Matheis

Origin and regional significance of late Precambrian and early Palaeozoic granitoids in the Pan-African belt of Somalia

Received: 20 July 1993 / Accepted: 18 May 1994

Abstract Granitoids within the Precambrian basement of north-eastern and southern Somalia are subdivided on the basis of geology, geochronology and petrology into three different assemblages. The post-kinematic assemblage in north-eastern Somalia ($\approx$ 630 Ma) comprises granodiorites and granites which belong to a medium-K calc-alkaline suite. Average initial Sr, Nd and Pb isotopic ratios [$Sr_i = 0.7048$, $\varepsilon_{Nd} = -1.8$, $^{206}Pb/^{204}Pb(i) = 17.704$ and $^{207}Pb/^{204}Pb(i) = 15.611$] indicate that these melts were derived from a mantle or juvenile crustal source with only slight involvement of pre-existing crust as a contaminant. Two different assemblages are found in southern Somalia. The older assemblage is composed of crustal anatectic, synkinematic, parautochthonous granites ($\approx$ 600 Ma) related to amphibolite facies retrogression of an intensively reworked pre-Pan-African crust [$Sr_i = 0.7100$, $\varepsilon_{Nd} = -8.4$, $^{206}Pb/^{204}Pb(i) = 15.403$ and $^{207}Pb/^{204}Pb(i) = 15.259$]. These monzo- and syenogranites are moderately potassic and peraluminous. The younger assemblage ($\approx$ 470 Ma) consists of post-kinematic monzonites to syenogranites with A-type affinities. Initial Sr, Nd and Pb isotopic data for this metaluminous assemblage [$Sr_i = 0.7114$, $\varepsilon_{Nd} = -13.1$, $^{206}Pb/^{204}Pb(i) = 16.913$ and $^{207}Pb/^{204}Pb(i) = 15.512$] indicate a significant lower crustal component but, however, also a mantle signature. The late Proterozoic to early Palaeozoic granitoids in Somalia thus express contrasting regimes, characterized by strong juvenile input in the north, close to the Arabian–Nubian Shield, whereas intense crustal reworking with little addition of juvenile material prevailed in the south. Somalia was definitively not a cratonic area during the Pan-African, but a zone of high crustal mobility.

Key words Pan-African · Granitoids · Geochronology · Isotope geochemistry · Mozambique Belt · Somalia

J.-L. Lenoir (✉) · J.-P. Liégeois
Département de Géologie, Musée royal de l'Afrique centrale, B-3080 Tervuren, Belgium, FAX: 32-2-7695432

D. Küster · A. Utke · G. Matheis
SFB 69, TU Berlin, Ackerstrasse 71, D-13355 Berlin, Germany

A. Haider
Department of Earth Sciences, Open University, Milton Keynes, MK7 6AA, UK

Introduction

The Precambrian basement of the Horn of Africa (Fig. 1) is, by its geographical position, a key area for the geology of East Africa. It is located between the mainly juvenile greenschist facies assemblages of the Arabian–Nubian Shield (ANS) to the north and north-west (Egypt, Sudan, Saudi Arabia) and the polycyclic high grade metamorphic terrains of the Mozambique Belt to the south (Kenya, Tanzania, Mozambique), both of Pan-African age (950–550 Ma).

Several workers (D'Amico et al., 1981; Warden and Horkel, 1984) have emphasized the broad structural and lithological similarities between the Somalian basement and the terrains located to the south. It was therefore postulated that the Precambrian of Somalia formed the north-eastern branch of the Mozambique belt (Fig. 1). The main trunk of the Mozambique Belt is seen to extend from Mozambique to Sudan through western Ethiopia, whereas the north-eastern branch is thought to extend to Yemen and south Arabia. The two branches are separated by the Adola belt of oceanic affinity (greenstones and metamorphosed ultrabasic rocks; Warden and Horkel, 1984; Worku and Yifa, 1992), a belt which widens northwards to form a volcanic arc basin when passing into the ANS.

Although the geology of the ANS has been extensively studied and debated (e.g. Gass, 1977; Greenwood et al., 1980; Stern, 1981; Stoeser and Camp, 1985), the relationship between the ANS and the Mozambique Belt remains unclear. This results from more severe deformation and metamorphism in the Mozambique Belt, combined with the diversity and complexity of the rock assemblages encountered along the orogen strike. Even

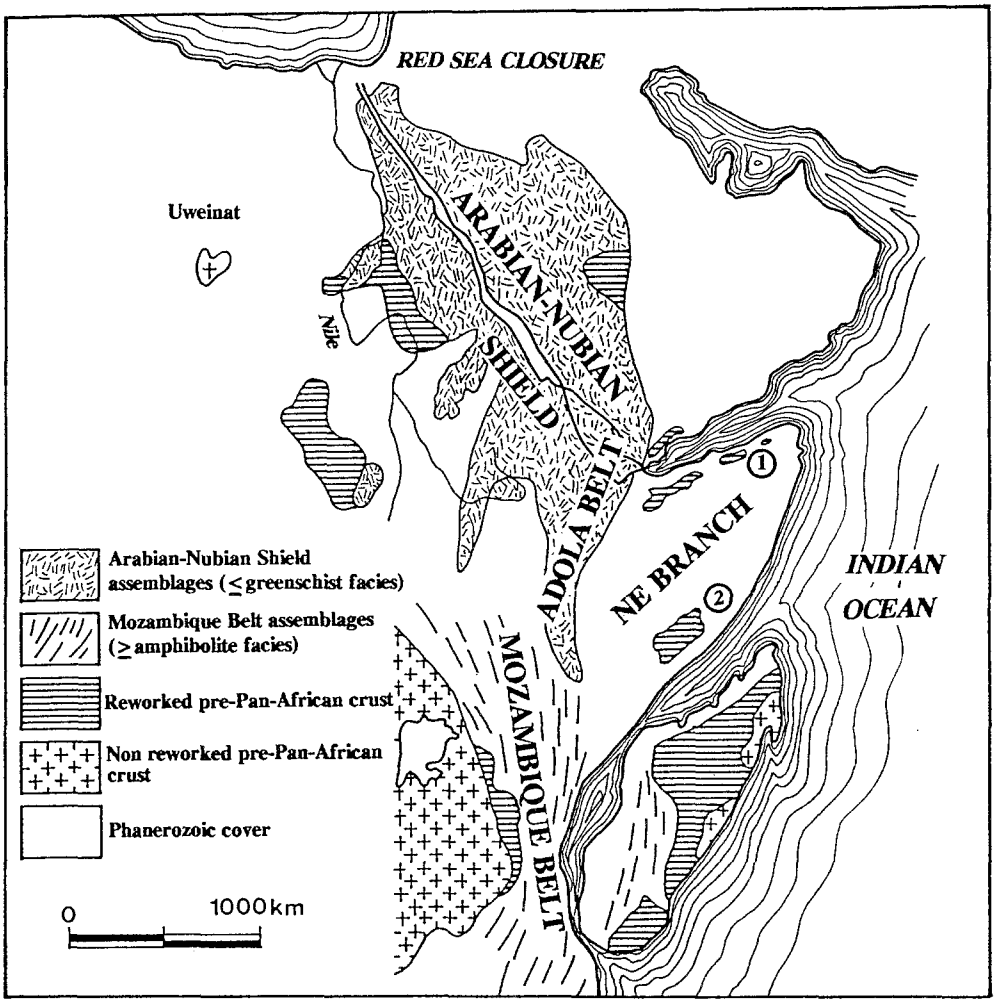

Fig. 1. Geological sketch map of eastern Africa (modified after Berhe, 1990; Harms et al., 1990; Pinna et al., 1993). Circled numbers refer to exposed Precambrian basement of northern (1) and southern (2) Somalia

the nature of the belt remains controversial. Early models refer to ensialic development with the involvement and reworking of possible Archaean crust (Kröner, 1977; Almond, 1983). Later models are based on the recognition of a complete Wilson cycle and assume the existence of a cryptic suture matching a continental collision stage (Shackleton, 1986; Burke and Sengör, 1986; Key et al., 1989). Collision along the Mozambique Belt suture would have led to the final amalgamation of Gondwana at $\approx$ 600 Ma (Dalziel, 1992).

The aim of the present study is to draw a comparison between the late granitoids of north-eastern and southern Somalia by means of field observations, geochronological and geochemical results and to formulate some new constraints on the development of the Somalian basement during the Late Precambrian and Early Phanerozoic.

Geological setting

Northern Somalia

Precambrian basement (Fig. 2) crops out in northern Somalia within a 580 km long east–west oriented strip fringing the southern coast of the Gulf of Aden. It is unconformably overlain by a thick Mesozoic to Cenozoic sedimentary cover. The topography of the coastal range and thus the location of basement occurrences arise from uplift and block-faulting developed during the formation of the Gulf of Aden (Eocene–early Oligocene; Abbate et al., 1987). The Precambrian of northern Somalia comprises four main units (Fig. 2): the basement complex; two metavolcanic units (Maydh belt and Abdulkadir complex); and the supracrustal Inda Ad Group. These units are intruded by late- to post-kinematic granitoids.

Basement complex

This consists mainly of a metasedimentary sequence that underwent a high grade metamorphism comparable with that affecting other parts of the Mozambique belt. Marble horizons are interbedded with quartzites, various schists and subordinate amphibolites (Daniels, 1965). The whole basement association has been subjected to a polymetamorphic evolution and an intense reworking during the Pan-African (D'Amico et al., 1981; Kröner et al., 1989). Granitic gneisses, often described as 'mantled gneiss domes' (e.g. Warden, 1981), are widely distributed throughout the basement. The main structural trend is

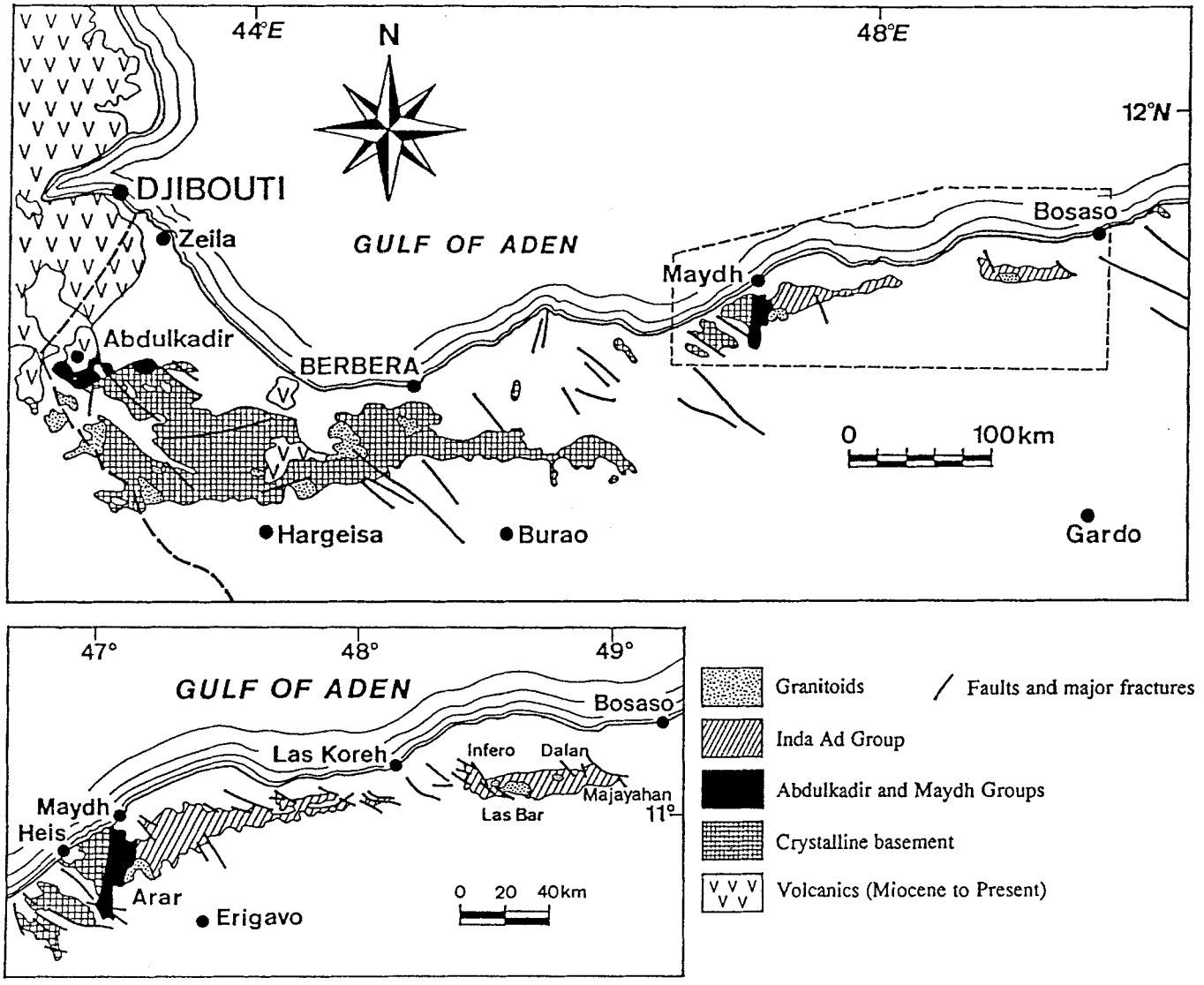

Fig. 2. Geological sketch map of northern Somalia (modified after Merla et al., 1973)

east–west within the western part of the basement, but eastwards these folds swing into a north-easterly alignment. Extensive migmatization and mobilization of quartzo-feldsphatic material have produced intricate, commonly nebulitic structures of variable trends.

Inda Ad Group

The high grade metamorphic rocks of the basement complex are overlain in north-eastern Somalia by a thick sedimentary sequence which was folded and metamorphosed under lower greenschist facies conditions (Warden and Horkel, 1984; Utke et al., 1990). The Inda Ad Group, 210 km wide, is essentially arenaceous in composition with subordinate carbonate beds. The regional structure is characterized by long wavelength open folds with subvertical axial planes (Greenwood, 1960). To the west, folds become progressively tighter and finally evolve to isoclinal folds, with a general westward vergence (Mason and Warden, 1956). This suggests thrusting of the Inda Ad Group onto the Maydh belt and the basement complex to the west. However, the basal thrust has not been observed.

Maydh greenstone belt

This belt separates the Inda Ad Group from the basement complex. It consists of various sediments, microgabbros, tuffs and pillowed basalts, all metamorphosed to the greenschist facies. The metabasalts show chemical affinities with modern mid-ocean ridge basalts (MORBs) but, since ophiolitic associations are missing, the Maydh belt is believed to represent a rift basin with little input of oceanic crust (Utke et al., 1990).

Abdulkadir complex

This complex fringes the westernmost edge of the basement complex. It consists of mafic lavas, agglomerates of calc-alkaline character, with a greenschist

facies metamorphic overprint. This unit is thought to represent the active margin of the Adola volcanic arc basin (Warden, 1981).

Late to post-kinematic granitoid intrusions

These occur throughout northern Somalia. This study is restricted to those emplaced into the low grade supracrustal sequences of the Inda Ad Group. These intrusions are known as the Arar, Las Bar, Infero and Dalan plutons (Fig. 2). Composed mainly of granodiorites at Las Bar, of granites at Infero and Arar and of gabbro-diorites at Dalan, these circular to elliptical intrusions display discordant contacts characterized by hornfelses. These features, together with the permissive mode of emplacement, the steep plunge of contacts and the absence of internal foliation point to a high level post-kinematic emplacement. This indicates an important crustal relaxation phase which was probably associated with rapid basement uplift. Late pegmatites and hydrothermal quartz veins are found intruding shear-opened joints and tension gashes of the country rocks. Veins mineralized with cassiterite occur isolated at Majayahan (Fig. 2) or are spatially associated with gabbroic intrusives at Dalan. The Las Bar pluton, to which the Infero stock is a satellite, is the largest magmatic body (14×7 km) of north-east Somalia. It was emplaced into a large synformal structure of the Inda Ad Group. Weakly oriented microgranular quartz dioritic enclaves are abundant. Rounded in shape, they show sharp contacts with the granodioritic matrix. Hornfels enclaves are less common and are concentrated towards the margins of the pluton. Large angular xenoliths of country rocks are also preserved and appear generally stretched and net veined. At Infero, they are concentrically disposed. Under the microscope, the magmatic facies differ essentially by their proportions of normally zoned plagioclase, microcline, quartz, brown biotite and hornblende. The primary mineralogy is replaced: alteration of plagioclase to sericite and calcite and subsequent growth of epidote, chlorite and titanite. The existence of aplitic dykes and pegmatitic as well as carbonaceous fracture-fillings attest for a late hydrothermal stage.

Southern Somalia

The Precambrian basement of southern Somalia (Fig. 3) is exposed in numerous inselbergs rising out of the peneplain west of Mogadishu (the so-called 'Buur area').

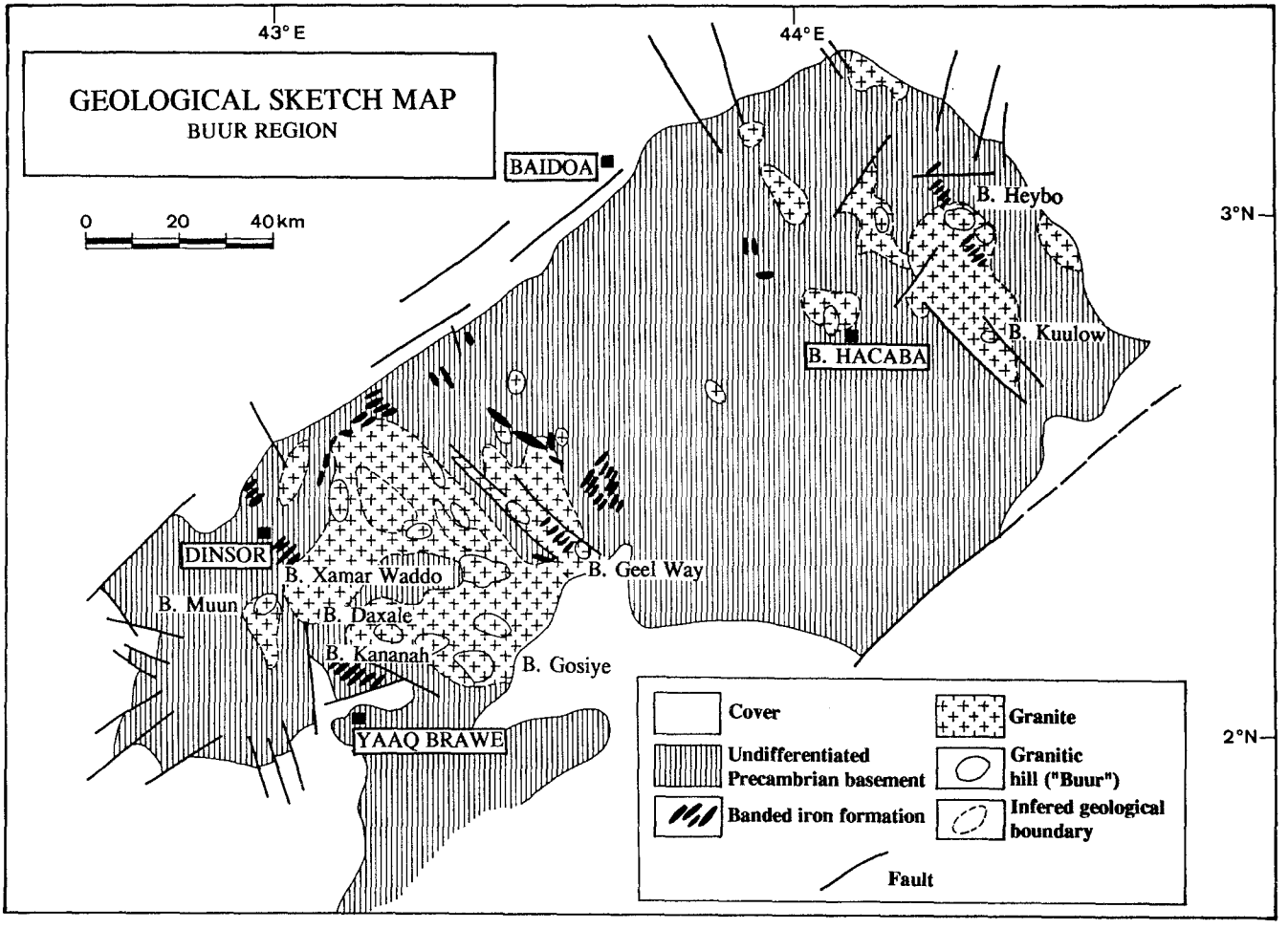

Fig. 3. Geological sketch map of southern Somalia

The Buur plain represents a deeply eroded, fault-bounded horst of Precambrian gneisses intruded by granitoids, which are overlain by Jurassic to Quaternary sediments.

Basement complex

This consists mainly of polycyclic metasedimentary rocks (including Banded Iron Formation or itabirite), ortho- and paragneisses with subordinate layers of amphibolite and calc-silicate rocks. The meta-igneous rocks consist of mafic and ultramafic rocks (pyroxenites, hornblendites and tremolitites), dioritic gneisses, migmatitic gneisses (ranging from tonalitic to granitic compositions) and metavolcanic rocks, whereas the metasedimentary rocks consist of sillimanite quartzites, garnet sillimanite gneisses, marbles, calc-silicates and hypersthene magnetite quartzites. The whole sequence has been subjected to granulitic metamorphism followed by a retrograde amphibolite metamorphic overprint coeval with migmatization (Haider, 1989). The Buur area can be divided into two sectors (Küster et al., 1990a): the north-eastern sector is characterized by a dominant NW–SE trending foliation associated with subisoclinal folds (S1). Locally, the north-west trending foliation is refolded (S2) along roughly north-easterly trending axes. The south-western sector is structurally more complex. The foliation is essentially WNW–ESE trending (S1), but is often severely refolded (S2) during the second phase with NE–SW associated structures. This second tectonic phase is probably linked to amphibolite facies retrogression, migmatization and widespread granitization. The first tectonic phase (S1) is most probably contemporaneous with the granulitic event.

Syn- to late kinematic granites (SW sector, Fig. 3)

These granites crop out in several inselbergs (Daxale, Dinsor, Geel Way, Gosiye, Kananah, Muun, Xamar Waddo). They form rather small bodies and generally consist of leucocratic fine-grained monzo- and syenogranites. Each intrusion is characterized by a limited compositional range. Contacts between magmatic rocks and the surrounding migmatized gneisses can be either diffuse, concordant ('sheet-like intrusions') or discordant. The widespread internal deformation (penetrative foliation) indicates a syn-to late kinematic setting for both granites and migmatization. Basement inclusions, particularly abundant, are concentrated towards the border of the plutons. They include mafic pods or refractory assemblages (magnetite-bearing quartzite), magnetite spots and schlieren, with all transitions. These inclusions are interpreted as restites and, together with the general leucocratic nature of the host granites, suggest a crust-dominated origin. However, as these granites were probably not generated by *in situ* remobilization of the gneissic country rocks, they are quoted as parautochthonous. The Daxale granitic intrusion is a small circular leucocratic body, rimmed by migmatites and passing laterally into a thick succession of biotite-rich paragneisses. It is floored by the surrounding migmatites, which suggests a sheet-like mode of emplacement. The rock is essentially composed of quartz, microcline and plagioclase (An 27–37). Clinopyroxene is present, often zoned, and retrogressed to green amphibole. Garnet (andradite variety) is restricted to some samples but may constitute about 5% of the rock. It is commonly destabilized and intimately associated with magnetite. The accessory minerals are represented by magnetite, haematite, ilmenite, apatite, monazite and zircon. Muscovite, calcite, titanite and chlorite are the main secondary minerals. Biotite is absent from the granite, but is found in the aplitic and pegmatitic dykes.

Post-kinematic granitoids (NE sector, Fig. 3)

These granitoids are diversified, ranging in composition from monzonites to syenogranites, containing both K-feldspar porphyritic and coarse-or fine-grained equigranular varieties. They were discordantly emplaced into the high grade basement at a shallower crustal level than the synkinematic group. Locally, a weak foliation of magmatic origin is induced by discontinuous layers of biotite or amphibole flakes and by preferred orientation of K-feldspar megacrysts. Xenoliths of amphibolite and gneiss are angular, vary in size and are concentrated towards the margins of the intrusions. Cogenetic enclaves occur only locally. They are mostly elongated microgranular lenses with a bulk composition similar to its plutonic host rock (microgranite). The Buur Heybo porphyritic monzogranite is characterized by weakly perthitic K-feldspar megacrysts (centimetre size), which are partly transformed into microcline within a quartzofeldsphatic matrix. Plagioclase (albite–oligoclase) is rarely zoned by contains numerous biotite and quartz inclusions. The ferromagnesian minerals are green–brown biotite and green amphibole relics. The Buur Hacaba monzo- and syenogranites are more leucocratic than the porphyritic variety and are characterized by isotropic and equigranular structures. Different generations of dykes can be distinguished. Microscopically, these granites are made up of quartz, often saussuritized plagioclase (albite–oligoclase), weakly perthitic microcline and green–brown biotite. A later crystallization phase is represented by quartz and feldspar symplectites. The accessory minerals are zircon, apatite, oxides and titanite.

Analytical procedures

Geochemical analysis were carried out at the Technical University of Berlin. Concentrations of major and trace elements for granitoids from northern Somalia were determined by atomic spectrometry techniques [flame atomic absorption spectrometry (AAS), flame atomic emission spectrometry (AES) and inductively coupled plasma (ICP) AES]. International rock standards with

recommended working values from Govindaraju (1984) were used for correction (for more details, see Küster, 1990). Compositions of granitoids from southern Somalia were determined by X-ray fluorescence spectrometry. The rare earth element (REE) contents were determined separately by ICP-AES after ion-exchange separation. Geochemical data are listed in Table 3.

The isotopic measurements (Pb, Sr, Nd) were carried out at the Belgian Centre of Geochronology (MRAC-ULB), except for some additional Rb–Sr analysis, which were carried out in Clermont-Ferrand, France. U–Pb isotopic compositions were measured on single Re filament with a Finnigan MAT 260 mass spectrometer by the H_3PO_4–silica gel technique. All results were corrected for mass fractionation (0.13% per amu) on the basis of the NBS 981 Pb standard. Sr isotopic compositions have been measured on Re double filament with a Finnigan MAT 260 and Nd isotopic compositions on triple Ta–Re–Ta filament with a Fisons VG Sector 54 mass spectrometer. The $^{87}Sr/^{86}Sr$ value of NBS 987 standard (normalized to $^{86}Sr/^{88}Sr = 0.1198$) during the course of this study was 0.710221 ± 0.000019 and the $^{143}Nd/^{144}Nd$ value of Merck Nd standard (normalized to $^{146}Nd/^{144}Nd = 0.5119$) was 0.512740 ± 0.000005. For additional details, see Tables 1, 2 and 6.

Geochronology

North-eastern Somalia

The Las Bar granodiorite was investigated with the U–Pb method; two distinct morphological populations of zircons were recognized in this intrusion. The first population, by far the most abundant, is interpreted as purely magmatic. It consists of elongated transparent crystals rich in minute inclusions. Electron microprobe investigations revealed inclusions of quartz, K and Na feldspars, acicular apatite and crystals of magnetite, but no inherited cores. The second population is composed of pinkish bipyramidal metamict crystals, which are xenocrysts or inherited zircons (see below). Four homogeneous, magnetically sorted fractions of magmatic zircons were selected as well as one metamict zircon fraction and one titanite fraction. The results are shown in Table 1. The magmatic fractions (Fig. 4a) define a discordia with an upper intercept of 626 ± 11 Ma and a lower intercept of 64 ± 40 Ma. The titanite fraction gives a $^{207}Pb/^{206}Pb$ age of 548 Ma, whereas the fraction of metamict zircon yields a $^{207}Pb/^{206}Pb$ age of 987 Ma. The lower intercept near the origin for the Las Bar discordia probably corresponds to a recent Pb loss (chemical weathering) or to a continuous lead loss. The imperfect alignment of the fractions probably reflects a disturbance of the U–Pb system after crystallization. This could be correlated with the thermal event recorded by the titanite. As the zircons selected are purely magmatic in appearance (no core or overgrowth observed), the fractions scattering can hardly be due to inheritance.

As the Las Bar granodiorite is post-kinematic, the U–Pb age (626 ± 11 Ma) of the magmatic zircons is interpreted as the emplacement age. This age constitutes an upper limit for deposition and folding of the metasedimentary Inda Ad Group. Moreover, it is probably also an upper limit for the Maydh greenstone belt, which is likewise intruded by plutons of this type. The inferred late Proterozoic age for the Inda Ad group can be compared with that of the similar Ghabar Group in South Yemen (Greenwood, 1961). The metamict zircon fraction of the Las Bar pluton indicates the participation of a crustal component probably much older than 1000 Ma in the genesis of this granodiorite.

The emplacement age of 626 ± 11 Ma is older than previous mineral age determinations on the Las Bar and Arar plutons. K–Ar age determinations on biotite gave ages around 515 Ma (Snelling, 1963), whereas Rb–Sr age determinations based on mineral pairs (biotite–feldspar) from the Arar granite yielded ages around 500 Ma (Abbate et al., 1985). Titanite is a mineral known to have a nearly concordant behaviour, but also to have a lower closure temperature for Pb isotopes than zircon. The titanite fraction ($^{207}Pb/^{206}Pb$ age of 548 Ma) is in agreement with the biotite mineral ages. The high level emplacement of the Las Bar pluton excludes the possibility that these ages are magmatic cooling ages. By contrast, the development of secondary epidote, titanite, muscovite and sericite suggest that these U–Pb titanite and Rb–Sr mineral ages are linked to a thermotectonic phase accompanied by fluid circulation in the 550–520 Ma period. This thermotectonic episode could be associated with the development of large pegmatitic and hydrothermal systems in the surroundings. Rb–Sr data on early formed muscovites from the Majayahan pegmatites have revealed even younger ages in the range 470–460 Ma (Küster, in press); it is suggested that these pegmatites were subjected to partial open system behaviour in relation to unsystematic fluid activity and slow cooling histories.

Southern Somalia

Three zircon fractions and one titanite fraction of the Daxale synkinematic granitic pluton have been analysed by the U–Pb method. The zircons gave a lower intercept at 553 ± 18 Ma and an upper intercept of 2515 ± 44 Ma (Fig. 4b). The Rb–Sr method applied to the same granite (Fig. 4c; Table 2) yielded only an errorchron (655 ± 52 Ma, 0.7083 ± 0.0024, 6 WR, MSWD = 13.9). Only four samples are satisfactorily aligned and give similar results (637 ± 51 Ma, 0.7087 ± 0.0023, 4 WR, MSWD = 1.78). Enclosing migmatites give a better alignment and the same age within error limits: 601 ± 21 Ma, 0.7112 ± 0.0007, 6 WR, MSWD = 4.08 (elimination of sample 4e leads to 594 ± 21 Ma, 0.7111 ± 0.0007, 5 WR, MSWD = 0.25). Omitting the three outliers, a common isochron can be calculated and yields 595 ± 17 Ma, 0.7109 ± 0.0006, 9 WR, MSWD = 1.35. The poor definition of the granite isochron and

Table 1. U–Pb isotopic data from Somalian granitoids

Fraction No.	Size (μm)	Magnetic properties°	Weight (mg)	Concentrations			Atomic ratios					Ages (Ma)		
				U (ppm)+	Pb (ppm)+	Pb rad (%)+	$^{206}Pb/^{204}Pb$§	$^{208}Pb/^{206}Pb$§	$^{207}Pb^*/^{235}U$$	$^{206}Pb^*/^{238}U$$	$^{207}Pb^*/^{206}Pb^*$$	$^{207}Pb^*/^{235}U$	$^{206}Pb^*/^{238}U$	$^{207}Pb^*/^{206}Pb^*$
Las Bar granodiorite														
Magmatic zircons														
1	106–150	−4° M	3.63	560	45	97	2139 ± 98	0.1500	0.6496	0.0764	0.06170	508	474	664
2	106–150	−5° M	2.18	594	54	96	1628 ± 56	0.1548	0.7016	0.0854	0.05958	540	528	588
3	106–150	−6° M	2.60	572	50	96	1685 ± 22	0.1538	0.6934	0.0830	0.06055	535	514	623
4	106–150	−7° M	1.79	593	48	96	1395 ± 34	0.1700	0.6078	0.0748	0.05891	482	465	564
Zircon xenocrysts														
5	63–106	−4° M	1.36	755	61	96	1576 ± 24	0.1416	0.7531	0.0758	0.07201	571	471	987
Titanite														
6	106–150	+5° M	38.5	70	8	67	145 ± 1	0.3363	0.6258	0.0776	0.05851	493	480	549
Buur Daxale granite														
Titanite														
1	63–150	+5° M	0.5	91	19	68	106 ± 1	0.7536	0.6008	0.1048	0.04159	478	642	–
Magmatic zircons														
2	63–150	+1° M	2.33	52	11	85	256 ± 1	0.5195	1.9039	0.1342	0.10289	1082	812	1677
3	63–150	−1° M	2.99	52	11	95	855 ± 36	0.3694	2.7550	0.1675	0.11929	1343	998	1946
4	63–150	−3° M	4.69	38	8	94	780 ± 19	0.3480	2.6020	0.1597	0.11817	1301	955	1929
Buur Dur Dur granite														
Magmatic zircons														
1	106–150	+5° M	6.43	101	26	43	52.2 ± 0.1	1.0505	0.6816	0.0819	0.06025	528	508	615
2	106–150	+1° M	8.55	105	30	38	45.9 ± 0.2	1.1397	0.6525	0.0794	0.05933	510	493	588
3	106–150	−1° M	7.08	108	29	42	50.5 ± 0.1	1.0765	0.7121	0.0824	0.06275	546	510	698
4	106–150	−3° M	9.25	101	20	54	76.8 ± 0.3	0.7751	0.7650	0.0861	0.06427	577	533	755

° Indicated degree of tilt of Frantz isodynamic separator (1.5 A-25° slope), negative sign characterizes diamagnetic fractions.
+ Error on U/Pb ratio < 1%.
* Corrected for common lead (determined by K-feldspar analysis) and contamination (blanks < 200 pg).
§ Ratios corrected for isotopic fractionation only (0.13% per amu).
$ Ratios corrected for fractionation, blank and initial common Pb (error on $^{207}Pb/^{206}Pb$ < 0.1%).
* Radiogenic lead.
Chemical processes modified after Krogh (1973) and Lancelot (1975). The following disintegration constants were used (Steiger and Jäger, 1977): $^{235}U = 9.8485 \times 10^{-10}\,a^{-1}$; $^{238}U = 1.55125 \times 10^{-10}\,a^{-1}$.

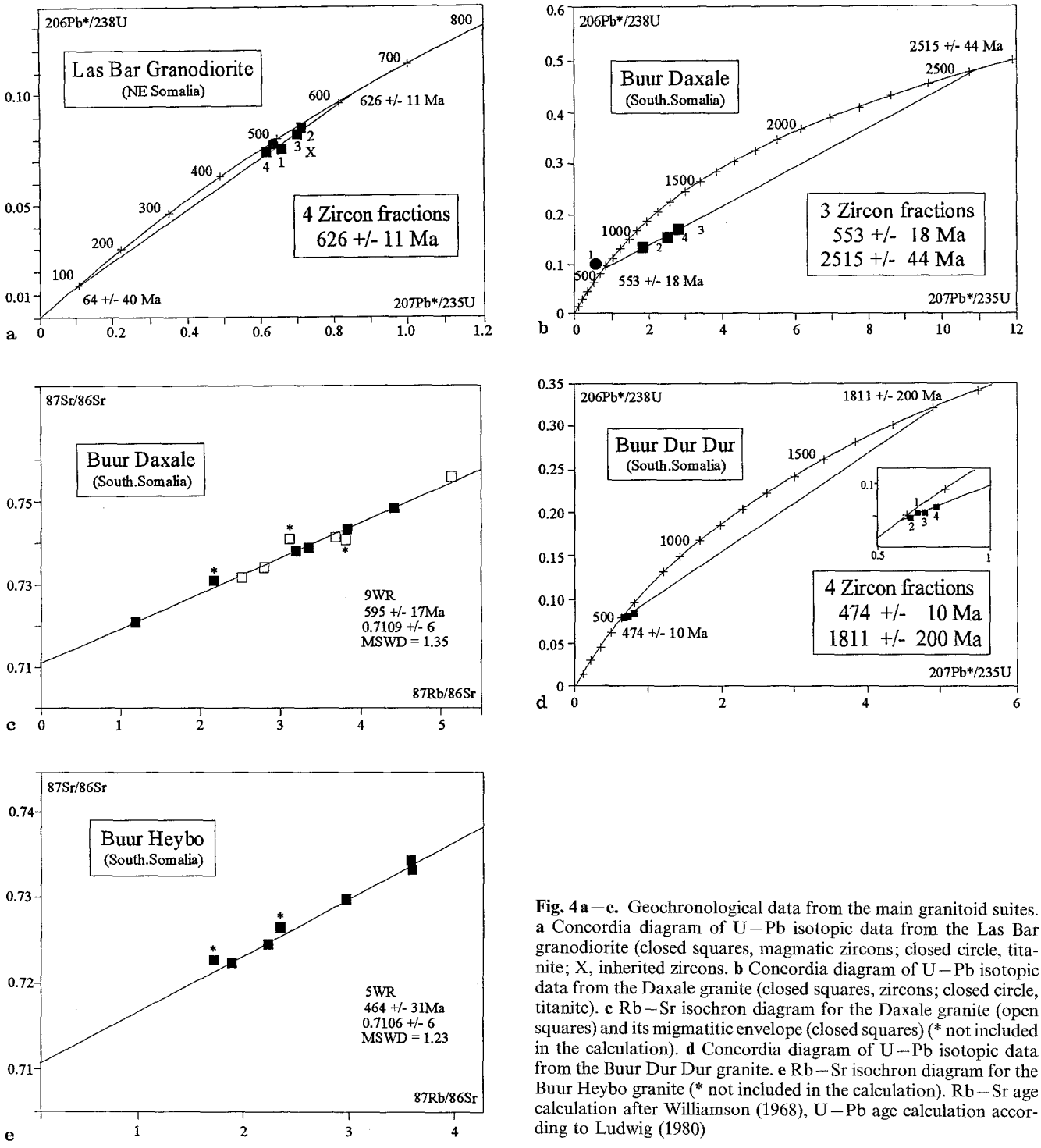

Fig. 4a–e. Geochronological data from the main granitoid suites. **a** Concordia diagram of U–Pb isotopic data from the Las Bar granodiorite (closed squares, magmatic zircons; closed circle, titanite; X, inherited zircons. **b** Concordia diagram of U–Pb isotopic data from the Daxale granite (closed squares, zircons; closed circle, titanite). **c** Rb–Sr isochron diagram for the Daxale granite (open squares) and its migmatitic envelope (closed squares) (* not included in the calculation). **d** Concordia diagram of U–Pb isotopic data from the Buur Dur Dur granite. **e** Rb–Sr isochron diagram for the Buur Heybo granite (* not included in the calculation). Rb–Sr age calculation after Williamson (1968), U–Pb age calculation according to Ludwig (1980)

the strong scattering in the isotopic characteristics for the studied samples can be correlated with the presence of xenocrysts or partly assimilated phases in the granite owing to its parautochthonous origin. The agreement between the Rb–Sr results on the granite and on the migmatites shows that the granite and its envelope have suffered intense geochemical exchange.

Taking into account the assigned errors, there is a discrepancy between U–Pb zircon (553 ± 18 Ma) and Rb–Sr WR results (595 ± 17 Ma). In the concordia diagram, the zircon fractions plot far from the lower intercept. This, combined with the possible effects of recent lead loss, may deeply affect the age calculation and its reliability. In consequence, we prefer to consider the Rb–Sr age as the emplacement age (more exactly, the closing age of the Rb–Sr isotopic system at the end of emplacement). This age also corresponds with the end of the regional deformation associated with amphibolite facies metamorphism and migmatization. The amphibolite facies event probably represents a retrogression

Table 2. Rb–Sr whole rock isotopic data from Somalian granitoids

Sample	Rb	Sr	$^{87}Rb/^{86}Sr$	$^{87}Sr/^{86}Sr$	$\pm 2\sigma$
Buur Heybo					
BH 1a	189	157	3.4950	0.73431	±7
BH 1b	160	288	1.6044	0.72313	±12
BH 2	175	228	2.2269	0.72722	±4
BH 3	153	208	2.1397	0.72461	±8
BH 4	185	153	3.5155	0.73327	±5
BH 5	194	196	2.8729	0.72969	±13
BH 7	188	305	1.7893	0.72256	±4
Buur Daxale					
BD 4a	97	84	3.3473	0.73924	±8
BD 4b	79	197	1.1573	0.72090	±7
BD 4c	102	94	3.1731	0.73775	±8
BD 4d	128	98	3.7930	0.74316	±9
BD 4e	62	83	2.1531	0.73095	±7
BD 4f	130	86	4.3997	0.74886	±11
BD 5a	129	102	3.6770	0.74114	±7
BD 5b	143	110	3.7935	0.74070	±8
BD 5c	92	96	2.7978	0.73411	±6
BD 5d	105	60	5.1113	0.75598	±12
BD 5e	74	69	3.1249	0.74083	±8
BD 5f	93	109	2.4968	0.73177	±7

Rb and Sr concentrations were measured by X-ray fluorescence. The error on the Rb/Sr ratio is less than 2%. Decay constant for ^{87}Rb is 1.42×10^{-11} a^{-1} (Steiger and Jäger, 1977).

phase of an earlier granulite facies metamorphism which has been dated at ≈ 650 Ma (U–Pb zircon; Lenoir and Haider, 1990). The upper intercept (2515 ± 44 Ma) suggests a late Archaean protolith for this anatectic granite.

The Buur Dur Dur post-kinematic granitic pluton (a member of the Buur Hacaba suite) was dated by the U–Pb zircon method, yielding a lower intercept of 474 ± 10 Ma and an upper intercept of 1811 ± 200 Ma (Fig. 4d). The remarkably low $^{206}Pb/^{204}Pb$ ratios are probably linked to the high degree of discordance of the zircons. However, the results for the four fractions are coherent. The adjacent Buur Heybo granite was sampled for Rb–Sr age determination (7 WR). Most samples are porphyritic, except samples of microgranitic enclaves (samples BH 1b and BH 2). The isotopic compositions of these two samples, which may not be strictly cogenetic, are plotted in Fig. 4e, but were not considered in the final calculation. The Buur Heybo pluton yielded a Rb–Sr isochron (5 WR, 0.7106 ± 0.0006, MSWD = 1.23) with an age of 464 ± 31 Ma (Fig. 4e).

The zircons from Buur Dur Dur plot very near the concordia and date unambiguously the emplacement of this high level pluton (474 ± 10 Ma). Moreover, the age is identical within error limit with the Rb–Sr age (464 ± 31 Ma). The post-kinematic magmatism in southern Somalia is thus of middle Ordovician age. The upper intercept (1811 ± 200 Ma) constitutes a minimum age for older crustal material involved in the genesis of these granites. The early Phanerozoic magmatic event could be linked with the Pan-African tectonothermal episode originally defined by Kennedy (1964), a concept essentially based on mineral ages. However, it also falls in the age range of within-plate granitoid associations in Sudan (Harris et al., 1983) and is contemporaneous with the activation of late shear zones (Sacchi and Zanferrari, 1987) and the development of pegmatitic–hydrothermal systems (Küster et al., 1990 b) in northern Somalia. A link with the 'Taconic phase', and with the Caradoc deformation and epeirogenesis (Fabre, 1988) could also be advocated. Whatever age is assumed for the synkinematic granitoids and for the amphibolite facies metamorphism, a time gap of about 100 Ma is shown between the two granitoid groups of southern Somalia, suggesting that no genetic link exists between them.

Geochemistry

Three groups of granitoids were investigated during this study: the northern Somalian post-kinematic group (NI), the southern Somalian syn- to late kinematic group (SI) and the southern Somalian post-kinematic group (SII). In the QP diagram (Debon and Le Fort, 1983), chemical compositions of the three groups show different trends (Fig. 5a). The different evolution paths of the granitoid series of Lameyre and Bowden (1982) have been added to the diagram. The NI group belongs to a classical calc-alkaline series of predominantly granodioritic compositions; the SI group is restricted to the granite field corresponding with anatectic mobilisates; the SII group delineates a monzonitic high K calc-alkaline series.

From bulk chemistry (major and trace elements) and primary mineralogy, the Las Bar granodiorite (group NI) defines a metaluminous suite. The Na_2O content, which is fairly constant through the range of compositions, is relatively high, together with the Sr, Ca and Ba contents (Table 3).

The synkinematic granitoids of southern Somalia (groups SI) form highly evolved, Sr-poor leucocratic rocks. These granites are moderately potassic and peraluminous. The differentiation index (DI) for these granites is markedly high (generally > 90) and the corresponding SiO_2 content varies from 72 to 79%. The high SiO_2 content may suggest a crustal origin for the SI granitoids. Nevertheless, these values are out of the range for classical leucogranites whose silica content rarely exceeds 76% (e.g. Didier, 1973). This either reflects the assimilation of extremely silica-rich material (e.g. quartzites as seen on outcrops) by the granitic melts or, with respect to the refractory nature of the quartzites, more probably the strong interaction of the solidifying granite with late to post-magmatic fluids.

The post-kinematic granitoids of southern Somalia (group SII) show a subalkaline trend (alkali-calcic character in the Peacock alkali–lime diagram) and show similarities with the 'Rapakivi' granitoid suite (Küster and Harms, 1991). Compositions range from monzonite (61% SiO_2) to leucocratic granite (76% SiO_2), always displaying a metaluminous character. The earliest magmatic phases are found in the porphyritic varieties of Buur Heybo, whereas the most evolved phases are related to Buur Hacaba. The Buur Heybo trend is characterized

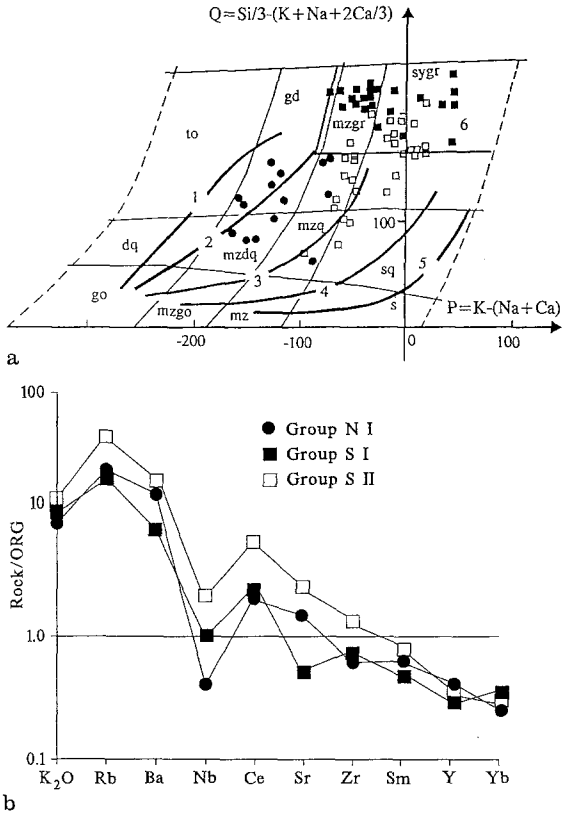

Fig. 5 a, b. Compositional diagrams of granitoid suites from Somalia. Closed circles, post-kinematic group N I (north-eastern Somalia); closed squares, synkinematic group S I (southern Somalia); open squares, post-kinematic group S II (southern Somalia). **a** QP classification diagram (Debon and Le Fort, 1983). The lines marked with numbers indicate the evolution paths of different granitoid series (after Lameyre and Bowden, 1982). 1, Calc-alkaline trondhjemitic ('Low K') series; 2, calc-alkaline granodioritic ('Medium K') series; 3, calc-alkaline monzonitic ('High K') series; 4, aluminous series of alkaline provinces; 5, alkaline and peralkaline series; and 6, anatectic mobilisates. **b** Oceanic ridge granite normalized diagram for selected elements, showing average element compositions of each granitoid suite. ORG data from Pearce et al. (1984). Normalized Sr abundances have been plotted assuming a ORG value of 110 ppm. Calculation of the normative factor was made according to the crystallizing assemblages and partition coefficients reviewed by Pearce et al. (1984)

by higher concentrations in compatible elements and by a significant enrichment in K_2O during differentiation. The agpaitic index gradually increases as a function of the SiO_2 content, but never exceeds 0.85.

Average element concentrations of the three Somalian granitoid groups, normalized to ocean ridge granite values (ORG; Pearce et al., 1984), are shown in Fig. 5 b. The three groups exhibit similar patterns of element distribution; the relative abundance decreases gradually with decreasing incompatibility from Rb to Yb. Common features are enrichment in mobile elements (K_2O, Rb, Ba) and light (L) REEs (Ce), negative Nb anomalies and low heavy (H) REE values. Group N I shows the most negative Nb anomaly, which may indicate an active plate margin setting. The negative Nb anomaly of group S I may be interpreted as a major crustal heritage, as such

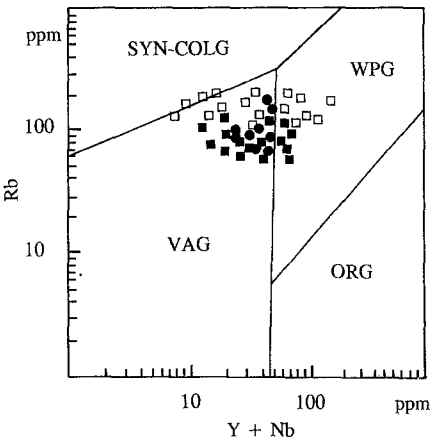

Fig. 6. Rb versus Y + Nb diagram. SYN-COLG, Syn-collision granites; WPG, within-plate granites; VAG, volcanic arc granites; ORG, ocean ridge granites; field boundaries from Pearce et al. (1984), symbols as for Fig. 5

anomalies are also geochemical characteristics of the deep continental crust of essentially intermediate composition (Taylor and McLennan, 1981). The post-kinematic group S II has the highest values for most of the elements.

Tectonic setting discrimination based on trace elements (Rb versus Y + Nb diagram; Pearce et al., 1984; Fig. 6) gave ambiguous results. The three groups always plot in two or more fields, predominantly in the volcanic arc granite (VAG) and syn-collision granite (syn-COLG), but sometimes also in the within-plate granite (WPG) fields. The scatter of data confirms the difficulty in applying this type of diagram to late orogenic granites (Pearce et al., 1984). The observed differentiation trends for group S II, together with the increased concentrations in high field strength (HFS) elements (Nb, Zr and Y) show that these granites share characters in common with suites emplaced in anorogenic settings (i.e. A-type granitoids). However, from the geochemical point of view, S II compositions deviate from average A-type granite compositions. In the diagram (Fig. 7) proposed to discriminate between A-type and orogenic granites (Whalen et al., 1987), the most differentiated members of group S II overlap with the compositions of felsic I- and S-type granites. It appears that the monzonitic magma had an alkaline affinity, but that the decrease in Zr, Nb, Ce and Y with increasing SiO_2 is more typical of calc-alkaline differentiation.

The REE concentrations are reported in Table 4; their normalized values are shown in relation to SiO_2 contents (Fig.8). The Las Bar granodiorite of group N I (Fig. 8 a) is characterized by relatively high total REE, strong LREE enrichment and slightly negative Eu anomalies, except for the most basic sample, which shows a positive Eu anomaly. Enrichment in all REEs follows the normal igneous differentiation trend. Plagioclase and amphibole are seen to dominate the fractionation process. The change from a slightly positive to a slightly negative Eu anomaly suggests increased fractionation of plagioclase during early stages of magmatic differentiation.

Table 3. Average chemical compositions and 1σ standard deviations of granitoids from north-eastern (group NI) and southern Somalia (groups SI and SII). Major element oxides in weight%, trace elements in ppm

	Las Bar (n = 24) N I		Infero (n = 6) N I		Buur Daxale (n = 4) S I		Buur Muun (n = 5) S I		Buur Geel Way (n = 5) S I		Buur Kanannah (n = 5) S I		B. Xamar Waddo (n = 4) S I		B. Heybo porph. (n = 4) S II		B. Heybo equig. (n = 7) S II		B. Hacaba (n = 10) S II	
Elements	Average	(σ)	Average	(σ)	Average	(σ)	Average	(σ)	Average	(σ)	Average	(σ)	Average	(σ)	Average	(σ)	Average	(σ)	Average	(σ)
SiO_2	67.52	4.62	71.37	3.39	76.1	1.1	78.3	1.8	79.1	0.3	79.1	0.5	76.3	0.7	65.97	3.52	72.47	2.60	71.63	2.68
Al_2O_3	15.41	1.49	14.49	1.19	12.84	0.89	12.32	0.86	12.48	0.15	12.11	0.29	11.59	0.33	15.52	0.54	13.85	0.85	14.63	0.38
TiO_2	0.48	0.26	0.25	0.20	0.15	0.03	0.14	0.06	0.05	0.01	0.09	0.02	0.37	0.03	0.95	0.39	0.50	0.19	0.43	0.26
Fe_2O_3	3.46	1.71	2.05	1.30	1.98	0.57	1.73	0.27	1.04	0.12	1.44	0.08	4.14	0.54	4.78	1.63	2.79	1.07	2.52	1.17
MgO	1.39	0.94	0.41	0.52	0.29	0.20	0.15	0.12	0.01	0.01	0.01	0.01	0.22	0.11	1.11	0.41	0.55	0.23	0.54	0.31
CaO	2.69	1.32	2.35	0.88	0.59	0.17	0.44	0.24	0.36	0.07	0.40	0.08	0.58	0.18	2.71	0.60	1.27	0.47	1.65	0.43
Na_2O	4.05	0.35	3.85	0.37	2.85	0.31	3.71	0.30	4.04	0.27	3.9	0.16	2.51	0.32	3.95	0.10	3.06	0.36	3.71	0.29
K_2O	3.60	1.02	3.50	0.48	6.22	0.41	4.78	0.21	4.38	0.15	4.24	0.13	5.24	0.43	4.97	0.33	5.98	0.37	5.13	0.43
P_2O_5	0.15	0.07	0.10	0.05	0.07	0.03	0.03	0.02	0.02	0.01	0.01	0.01	0.04	0.02	0.35	0.19	0.11	0.07	0.13	0.09
Rb	104	46	86	7	112	20	125	24	89	4	87	4	83	9	162	23	193	5	170	29
Ba	670	262	854	369	492	196	273	260	177	109	270	156	595	6	1302	102	953	283	1132	291
Nb	19	12	8	3	9	3	20	5	7	2	17	3	11	2	28	10	32	9	31	20
Ce	70	40	69	27	90	37	89	36	45	18	62	44	73	30	223	82	381	76	228	125
Sr	214	106	210	58	89	17	47	32	14	3	22	8	99	14	304	50	202	71	295	68
Zr	183	67	182	52	275	151	339	46	196	25	276	17	424	49	497	154	503	174	353	233
Y	23	10	21	11	22	13	32	10	37	14	40	16	17	6	36	15	43	8	30	20

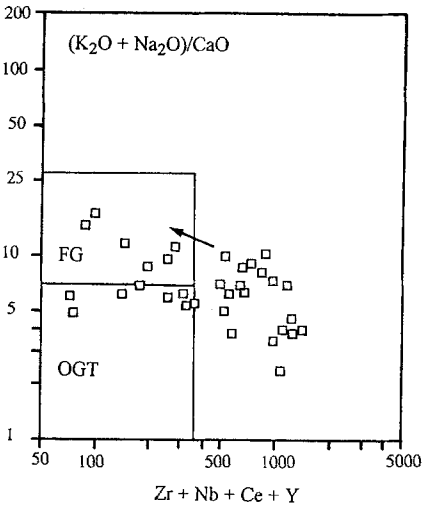

Fig. 7. $(K_2O + Na_2O)/CaO$ versus Zr + Nb + Ce + Y diagram for S II group. Field boundaries for A-type, fractionated felsic types (FG) and unfractionated I- and S-type granites (OGT) from Whalen et al. (1987). Arrow indicates differentiation trend

The REE patterns of the synkinematic group SI are shown in Fig. 8b. For the same range of SiO_2 contents (75–77%), the concentration of total REEs is highly variable, whereas the patterns are similar with steep LREE negative slopes, strong negative Eu anomalies and highly fractionated HREEs. This distribution of REEs departs significantly from expected chondrite-normalized profiles for classical anatectic leucogranites (e.g. Vidal et al., 1982), which are characterized by less pronounced REE fractionation and negative Eu anomalies. This confirms the importance of crystal–fluid partitioning processes during the evolution of the synkinematic SI group.

Buur Heybo and Buur Hacaba (post-kinematic group; SII, Fig. 8c) are characterized by high total REE concentrations and steep slopes for LREEs and HREEs. This suggests intermediate parental magmas, strongly enriched in REEs, confirming their A-type affinities. With progressing differentiation, total REE concentrations decrease and show a more pronounced negative Eu anomaly (Buur Hacaba). With increasing SiO_2, total REE contents behave coherently with incompatible trace elements (Fig. 7). This general decrease cannot be explained by fractional crystallization of major mineral phases, but shows the important role of accessory minerals. The high concentrations of REEs correlate with the abundance of minerals such as titanite, apatite and zircon seen in thin sections.

Isotope geochemistry

Representative samples from the different granitoid groups, possible source rocks of the SI group of southern Somalia (basement complex) and potential source rocks (mantle component, Maydh complex) of the Las Bar suite

Table 4. REE (ppm) compositions of representative samples from each granitoid association

	Post-kinematic group N I				Synkinematic group S I			Post-kinematic group S II			
	V11	Su82	GD3	Su20	74C	5F	27B	55E	54C	56A	51D
La	32.8	33.9	24.7	12.68	60.5	31.5	18.66	231	40.6	126	102
Ce	67.6	65.5	58.2	24.3	107.0	69.1	41.7	490	68.9	247	177
Pr	6.91	6.47	–	2.76	10.85	–	4.17	43.1	7.08	25.3	18.11
Nd	27.9	27.1	22.8	12.46	45.7	31.0	18.44	151	23.6	103	61.1
Sm	5.64	5.81	4.00	3.67	9.00	4.40	4.00	21.7	5.84	18.17	9.88
Eu	1.21	1.26	0.99	1.17	0.70	0.33	0.80	3.46	0.57	3.37	1.93
Gd	5.24	4.57	4.47	3.31	7.85	4.73	3.74	18.18	5.40	14.83	7.49
Dy	4.58	4.16	3.81	3.14	6.93	4.53	3.01	12.76	5.96	10.17	4.31
Ho	0.80	0.85	–	0.70	1.40	–	0.48	2.31	1.16	1.69	0.61
Er	2.35	2.48	2.51	2.24	3.76	2.73	1.38	6.39	2.95	4.54	1.74
Yb	2.37	2.05	1.90	1.80	4.14	2.49	1.24	5.81	2.89	3.82	1.49
Lu	0.37	0.32	0.29	0.28	0.58	0.37	0.21	0.77	0.36	0.54	0.18

(N I group) were analysed for Nd, Sr and Pb isotopic compositions (Tables 5 and 6). The results were compared with data from coeval granitoids of the ANS.

For the Las Bar granodiorite (group N I; Fig. 9), relatively low Sr initial ratios (Sr_i around 0.705) and slightly positive to moderately negative ε_{Nd} values were obtained (+0.8 to −3.4). This indicates a mantle origin of the granodiorite with the participation of pre-Pan-African continental crust or subducted sediments derived from such old crust. Further evidence for the involvement of old continental material is given by inherited Precambrian zircons (see under Geochronology). Crustal formation ages for the Las Bar granodiorite (Table 5) were calculated assuming a depleted mantle reservoir (T_{DM}) following De Paolo (1981). The T_{DM} ages between 1147 and 1600 Ma suggest the interaction of the magma with Early Proterozoic crust or even with Archaean material. The bulk chemistry, age range and tectonic setting of the Las Bar granodiorite suite are comparable with undeformed felsic plutons of the adjacent ANS. The vast majority of Sr and Nd isotope ratios of igneous rocks from the ANS (ophiolites and roughly coeval volcanoplutonic associations) suggest a mantle origin (e.g. Stern, 1981; Claesson et al., 1984; Harris et al., 1984). Nevertheless, there is a rough east–west variation in isotopic characteristics across the ANS (Harris et al., 1990). Igneous rocks with oceanic Nd signatures and similar emplacement and model Nd ages are restricted to the western terranes of Arabia and to the Red Sea Hills of Sudan. In Arabia and in Sudan, model Nd ages of late Proterozoic rocks increase gradually towards the east and the west, respectively. This corresponds with the increasing involvement of older crustal components in the formation of these magmas. According to Harris et al. (1990), most samples from Arabia have emplacement ages approximately equal to their model Nd ages (T_{DM}-t $\leqq$ 300 Ma). Samples characterized by T_{DM}-t $\geqq$ 900 Ma show continental Nd signatures, whereas T_{DM}-t values between 300 and 900 Ma are quoted as intermediate. The Las Bar pluton of north-eastern Somalia belongs to the latter group.

Granitoids from groups S I and S II (Table 5), although well discriminated on petrographical and geochemical

Table 5. Nd and Sr isotopic compositions from granitoid and basement samples

Sample	Sm (ppm)	Nd (ppm)	$^{147}Sm/^{144}Nd$	$^{143}Nd/^{144}Nd$	$\pm 2\sigma$	$\varepsilon_{Nd}(t)$	T_{DM}	Rb (ppm)	Sr (ppm)	$^{87}Rb/^{86}Sr$	$^{87}Sr/^{86}Sr$	$\pm 2\sigma$	$^{87}Sr/^{86}Sr(i)$
Granitoids													
N I													
Lb1	4.6	21.8	0.1276	0.512395	±26	+0.8	1147	74	315	0.6845	0.71133	±4	0.7052
Lb2	3.9	17.7	0.1332	0.512245	±15	−2.6	1506	86	280	0.8891	0.71261	±6	0.7047
Lb3	3.8	17.1	0.1343	0.512207	±40	−3.4	1600	86	297	0.8420	0.71205	±5	0.7046
S I													
BD5a	1.9	8.7	0.1320	0.511961	±19	−8.3	2017	129	102	3.6711	0.74114	±7	0.7097
BD5c	1.4	6.7	0.1263	0.511921	±36	−8.6	1954	92	96	2.7799	0.73411	±6	0.7103
S II													
BH7	2.7	23.0	0.0710	0.511601	±10	−12.7	1538	188	305	1.7860	0.72256	±4	0.7106
Dur2	17.2	127.5	0.0815	0.511590	±9	−13.5	1674	160	288	1.6098	0.72313	±3	0.7123
Maydh greenstones													
A2	4.2	13.3	0.1909	0.512869	±10	+5.0	1158	4	296	0.0371	0.70362	±3	0.7033
Basement complex													
B2	6.2	29.7	0.1262	0.511860	±14	−9.8	2060	66	150	1.2751	0.72438	±7	0.7135
4F	2.7	13.3	0.1227	0.511870	±24	−9.3	1963	130	86	4.3911	0.74886	±11	0.7113
B6	5.5	21.7	0.1532	0.512168	±40	−5.8	2207	73	88	2.4066	0.73546	±7	0.7149

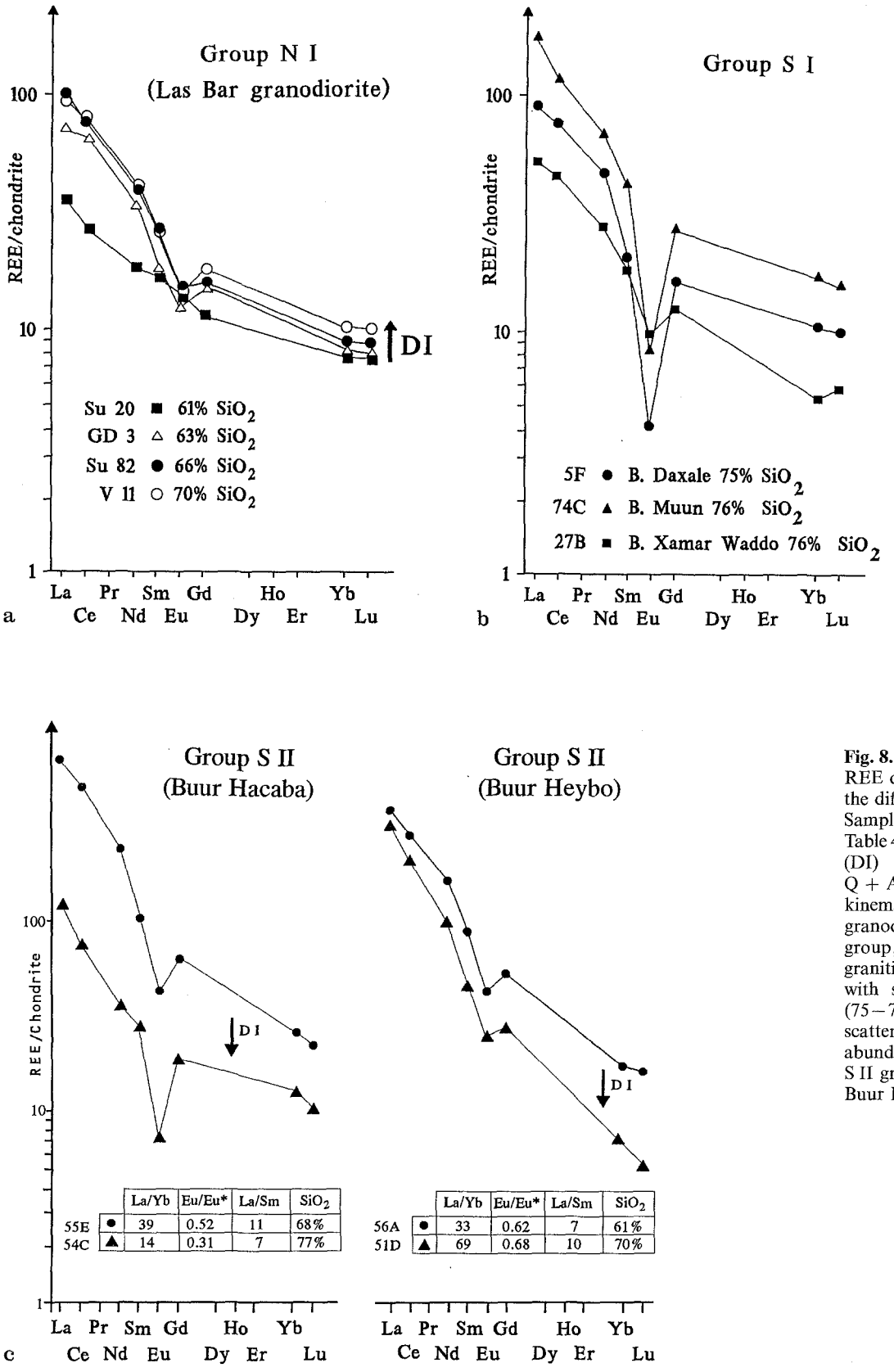

Fig. 8. Chondrite-normalized REE distribution patterns for the different granitoid groups. Sample numbers refer to Table 4. Differentiation index (DI) = normative Q + Ab + Or. **a** Post-kinematic N I group; Las Bar granodiorite. **b** Synkinematic SI group; patterns from different granitic intrusions (inselbergs) with similar SiO_2 values (75–77%). Note range and scattering of relative REE abundances. **c** Post-kinematic S II group; Buur Hacaba and Buur Heybo granite types

Table 6. Common lead data of K-feldspar and whole rock samples from granitoid associations and from the Basement complex. Initial compositions calculated back to the respective emplacement ages

Sample	U (ppm)	Pb (ppm)	$^{206}Pb/^{204}Pb$	$^{207}Pb/^{204}Pb$	$^{208}Pb/^{204}Pb$	$^{206}Pb/^{204}Pb(i)$	$^{207}Pb/^{204}Pb(i)$
Granitoids							
N I							
Lb2 (Kf)	0.02	42	17.766	15.577	37.742	17.764	15.577
Lb3 (Kf)	0.03	36	17.860	15.668	37.991	17.855	15.668
Lb4 (Kf)	0.07	47	17.849	15.658	37.943	17.840	15.657
Ar1 (Kf)	0.07	48	17.613	15.541	37.520	17.604	15.540
J8 (WR)	1.40	9	18.417	15.673	38.734	17.456	15.615
S I							
BDa4 (Kf)	0.06	16	15.265	15.233	35.441	15.243	15.232
5A (WR)	0.20	11	15.513	15.253	35.877	15.410	15.247
BM5 (WR)	0.96	7	16.343	15.345	37.222	15.557	15.298
S II							
BK1 (Kf)	< 0.01	69	16.736	15.422	37.308	16.736	15.422
BD2 (Kf)	< 0.01	47	17.010	15.556	37.665	17.009	15.556
BH5 (WR)	1.76	25	17.324	15.576	39.095	16.995	15.557
Basement complex							
BG3 (Kf)	< 0.01	65	15.287	15.250	35.482	15.286	15.250
BQ1 (Kf)	0.03	40	15.600	15.375	36.295	15.555	15.315

Ratios corrected for fractionation (0.13% per amu). Error on U/Pb ratios is in the 2% range, whereas between-run precisions are better than ±0.1% for the $^{206}Pb/^{204}Pb$ and $^{207}Pb/^{204}Pb$ ratios and better than ±0.15% for the $^{208}Pb/^{204}Pb$ ratios. Total blank values were in the ng range.

grounds, have Nd and Sr initial values in the same range (Fig. 9). However, samples from group S II are characterized by more negative ε_{Nd} and younger T_{DM} ages. The isotopic compositions of samples from group S I are close to those of basement samples at 600 Ma (Fig. 9) and the T_{DM} ages of both are similar, around 2 Ga. This indicates at least a substantial contribution of continental crust in the genesis of the parautochthonous granites. The T_{DM} ages furthermore indicate that the basement of southern Somalia is probably Palaeoproterozoic and not Archaean in age. Group S II samples have similar ε_{Nd} but lower Sr_i values than the basement at 470 Ma (Fig. 9). This indicates a lower crustal component depleted in Rb but not in Sm. Nevertheless, the younger T_{DM} ages of the granitoids (1538 and 1674 Ma; Table 5) indicate the participation of a component younger than the basement (2000 Ma), which was most probably the mantle. We therefore interpret the Nd – Sr isotopic signature of group S II to be the result of a mixture between the mantle and lower crustal components.

Fig. 9. ε_{Nd} versus Sr_i diagram for Somalian granitoids and possible source rocks. Isotopic characteristics are re-calculated to the ages indicated. Maydh tholeiitic basalts, mean isotopic composition (possible coeval depleted mantle source composition at 626 Ma, for more details see Utke et al., 1990); basement, high grade gneisses from the basement complex of southern Somalia

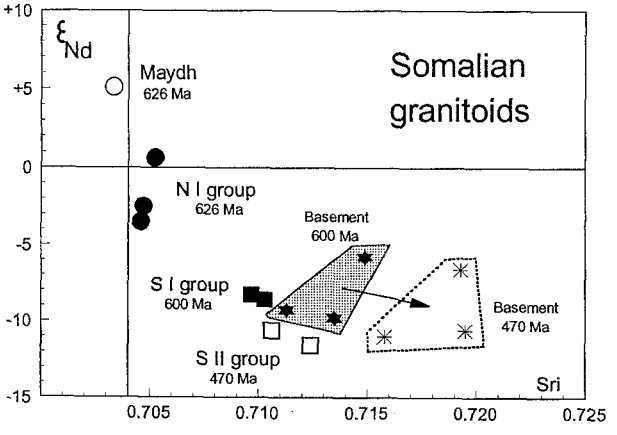

Pb isotopic compositions and U and Pb concentrations were obtained from nine K-feldspar concentrates and four whole rocks (Table 6). Isotopic compositions were corrected for radiogenic decay since crystallization (Table 6). Initial $^{207}Pb/^{204}Pb$ and $^{206}Pb/^{204}Pb$ ratios are plotted, together with Pb isotope data from the basement complex of southern Somalia (Fig. 10). Pb is a good isotopic tracer sensitive to crustal contamination and can be used to differentiate between lower crust, upper crust and mantle signatures (Stacey and Kramers, 1975; Doe and Zartman, 1979). Lower crust is characterized by severe U depletion under high grade to very high grade conditions, leading to significantly lower U/Pb ratios than those of the mantle. Consequently, lower crustal rocks have significantly less radiogenic Pb ratios than mantle-derived rocks (Moorbath et al., 1969; Gray and Oversby, 1972). The three groups of granitoids (N I, S I, S II) form separate fields in the $^{207}Pb/^{204}Pb$ versus $^{206}Pb/^{204}Pb$ diagram. The post-kinematic group of north-eastern Somalia (group N I) is the most radiogenic, whereas group S I constitutes the least radiogenic group, similar to the basement samples. Group S II occupies an intermediate position between these two fields. All groups plot along the orogene curve (Doe and Zartman, 1979) or along the evolution path proposed by Stacey and Kramers (1975). The most radiogenic group (N I) shows the lowest amount of crustal contamination. Its average initial Pb isotopic ratios (calculated at 626 Ma), corres-

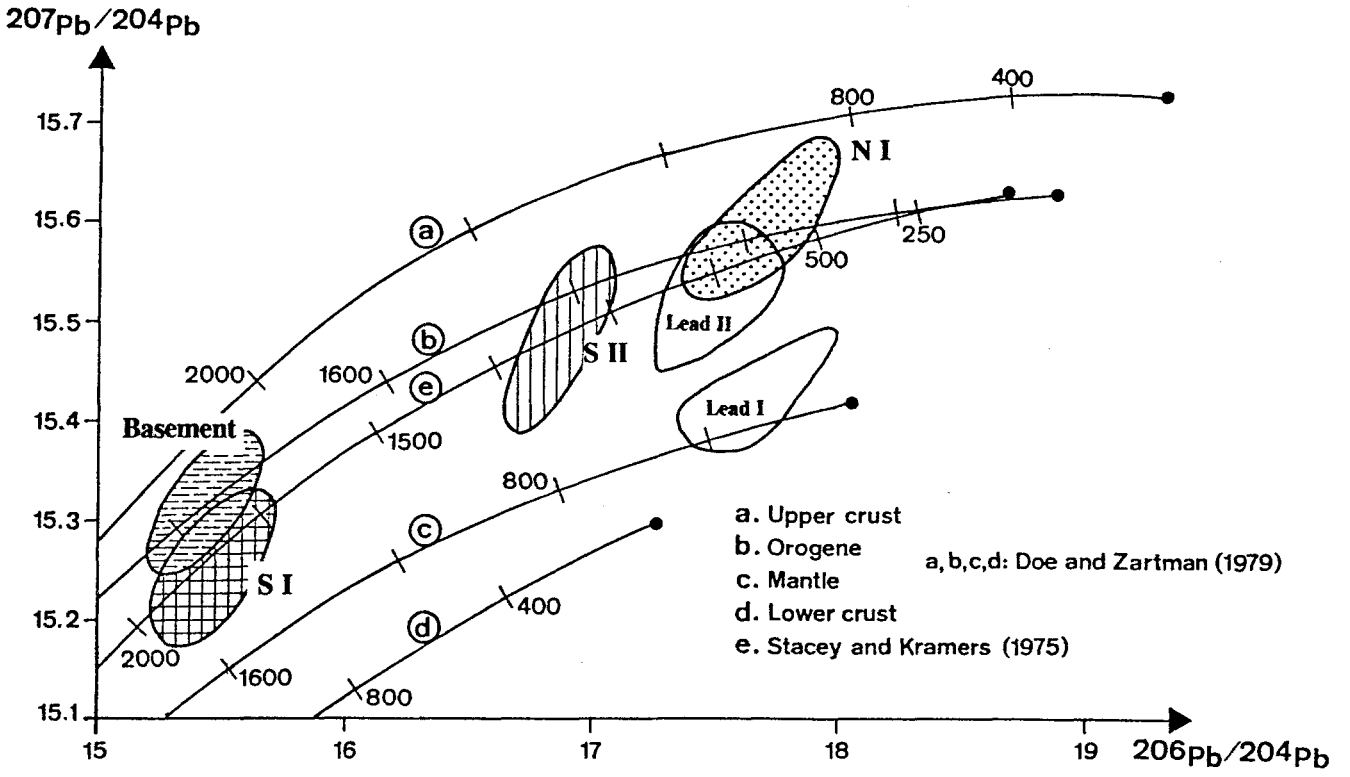

Fig. 10. Initial $^{207}Pb/^{204}Pb$ versus initial $^{206}Pb/^{204}Pb$ diagram for the three granitoid suites and the basement complex of southern Somalia. Fields correspond to the recorded range of variation for each group. Common lead data were obtained from feldspar concentrates and whole rock bulk analysis. Ratios were corrected assuming U decay and calculated back to the respective emplacement. For comparison, curves representative of different terrestrial reservoirs were drawn as proposed by the models of Doe and Zartman (1979) and Stacey and Kramers (1975). Graph also includes lead isotope data from the Arabian–Nubian Shield. Groups I and II are the compositional fields from Saudi Arabian galena (Stacey et al., 1980)

ponding to a $\mu 1$ ($^{238}U/^{204}Pb$) value of 8.3, are compatible with a mantle origin of the parental magma. After Zartman and Doe (1981), the upper mantle μ value at that time is ≈ 8.5, whereas the lower crust μ value is ≈ 6.3. The samples of the least radiogenic, synkinematic S I group plot close to the samples of the high grade gneisses of the basement complex. Pb compositions of the latter plot above the evolution line for the lower crust (Doe and Zartman, 1979) and $\mu 1$ values for granites and gneisses are generally higher than those of the lower crust at the time of emplacement. The rather high values of $^{238}U/^{204}Pb$ ratios of basement rocks suggest that the crust of southern Somalia is only moderately depleted in U and also in Rb. This indicates that the peraluminous synkinematic S I granites were generated by anatexis in the middle crust. Group S II samples (Fig. 10) show intermediate Pb isotopic compositions, significantly different from the samples of the synkinematic S I group. Pb isotopic compositions suggest that the metaluminous post-kinematic S II suite has a mantle origin with a significant contribution from the lower crust.

Pb isotopic data from the ANS are plotted in Fig. 10. The common lead data are divided into two main groups according to the results of Stacey et al. (1980). This two-fold common Pb distribution is based on a much larger data set than the three-fold representation of Harris et al. (1990), which is based on a limited number of Nd isotopic data. Nevertheless, both isotopic plots yield coherent distribution trends. Group I leads have oceanic (mantle) characteristics, whereas group II leads have incorporated a continental crustal component of at least Palaeoproterozoic age (Stacey and Stoeser, 1983). Granitoids from group N I are very close to the fields defined by crust-contaminated igneous rocks of the ANS (Lead II), which is not the case for the less radiogenic southern Somalian S I and S II granitoid groups.

Conclusions

Petrogenesis of granitoids

Field, geochronological and geochemical data enable recognition of three distinct 'late' granitoid phases in Somalia, which, from north to south, show contrasting evolution and tectonic settings.

In north-eastern Somalia, post-kinematic granodioritic to granitic plutons of calc-alkaline compositions were emplaced around 630 Ma, intruding the low grade supracrustal Inda Ad Group. These granitoids are mainly juvenile in origin and resemble the undeformed felsic plutons of the ANS. However, the north-east Somalian magmas have interacted with a pre-Pan-African crust which must be present at depth, indicating that before the

intrusion of the post-kinematic granitoids, the supracrustal Inda Ad Group was either deposited on, or tectonically emplaced onto, older basement. Evidence for the existence of old crust is given in the basement exposures of north-west Somalia, from where Kröner et al. (1989) reported granite–gneiss protolith ages between 1730 and 1820 Ma. After granitoid emplacement, sustained or renewed thermotectonic activities in the area resulted in fluid overprinting of the post-kinematic plutons between 550 and 500 Ma.

In southern Somalia synkinematic, ≈ 600 Ma old parautochthonous granites are genetically linked to migmatization and amphibolite facies retrogression following an earlier granulite facies metamorphism (≈ 650 Ma). These slightly peraluminous granites were derived from a Palaeoproterozoic crustal source, which was intensively reworked during the Neoproterozoic. Around 470 Ma the crust of southern Somalia was intruded by post-kinematic granitoids of metaluminous compositions that show some A-type characteristics. The mixed mantle–crustal sources of the SII group granitoids imply that their A-type characteristics (namely high HFSE and total REE contents) cannot simply be explained by the classical model of A-type granite formation (e.g. Whalen et al., 1987) in which enrichment of these elements arises from a second melting event of previously fused crust. The occurrence of the post-kinematic granites can be correlated with the broadly coeval emplacement of anorogenic syenitic to alkali granitic ring complexes in Sudan (Harris et al., 1983) and with activation of late shear zones and intense fluid circulation in northern Somalia (Küster, in press). The time gap of about 100 Ma between the emplacement of the synkinematic and the post-kinematic granitoid suites of southern Somalia precludes any genetic link between these two groups.

Regional significance

The Pan-African episode in Somalia represents intensive crustal reworking, reaching granulite facies conditions at ≈ 650 Ma (Lenoir and Haider, 1990). This age conforms with the age of granulite facies metamorphism in the Mozambique Belt between 750 and 650 Ma (e.g. Key et al., 1989; Mosley, 1993; Muhongo and Lenoir, 1994).

The Pan-African evolution of Somalia is broadly similar to that proposed for the highly metamorphosed basement rocks from southern Egypt and northern Sudan, west of the ANS (Fig. 1). There, the Pan-African episode involved considerable reworking of pre-existing crust of Palaeoproterozoic and/or Mesoproterozoic ages. Harms et al. (1990) have reported Pan-African ages (562–918 Ma) for basement gneisses, which were intruded by granitoids in the period between 560 and 620 Ma. Further west, the late Archaean basement of Gebel Uweinat was not affected by the Pan-African reactivation (Klerkx and Deutsch, 1977).

During the Pan-African the Palaeoproterozoic continental crust of Somalia separated orogenic domains (ANS and Adola belt to the north–west and west, and the Mozambique Belt to the south) from undisturbed Archaean or Palaeoproterozoic cratonic domains, which at that time, must have been located east of present day Somalia. Observations from Oman (Gass et al., 1990) have also led to the conclusion that before the break-up of Gondwana, the boundary between reactivated and undisturbed older Proterozoic crust was located between the Oman–Somalia region and the Archaean and middle Proterozoic terranes of the Bundelkhand and Aravelli areas of India. The protracted magmatic activity and metamorphism imply that Somalia was not a cratonic area during the Pan-African. Its evolution bears many similarities with that of the 'East Saharan Ghost Craton' in northern Africa (Black and Liégeois, 1993).

Acknowledgements Funded by German Research Foundation (DFG) within the framework of SFB 69. J. Klerkx (RMCA) is gratefully acknowledged for the initiation of the joint research program. We thank Mrs. Caen-Vachette from Université Blaise Pascal and CNRS, Clermont-Ferrand, for providing some Sr isotope data. Research carried out at the BCG was supported by an IRSIA grant for J. L. Lenoir. We thank R. J. Stern for stimulating comments and U. Harms and N. B. W. Harris for constructive critical reviews.

References

Abbate E, Bonazzi A, Dal Piaz GV, Del Moro A, Gosso G, Ibrahim HA, Savioli Mariani E (1985) Il settore occidentale dell'Unita di Inda Ad ed il granito di Arar (Somalia settentrionale). Quaderni Geol Somalia 8: 7–25

Abbate E, Bruni P, Fazzuoli M, Sagri M (1987) The continental margin of northern Somalia and the evolution of the Gulf of Aden. Proceedings of the Geosom 87 Meeting, Mogadishu, p 3

Almond DC (1983) The concepts of "Pan-African Episode" and the "Mozambique Belt" in relation to the geology of east and northeast Africa. Bull Fac Earth Sci, King Abdulaziz Univ 6: 71–87

Berhe SM (1990) Ophiolites in Northeast and East Africa: implications for Proterozoic crustal growth. J Geol Soc London 147: 41–57

Black R, Liégeois JP (1993) Cratons, mobile belts, alkaline rocks and continental lithospheric mantle: the Pan-African testimony. J. Geol Soc London 150: 89–98

Burke K, Sengör AMC (1986) Tectonic escape in the evolution of the continental crust. Am Geophys Union, Geodyn Ser 14: 41–53

Claesson S, Pallister JS, Tatsumoto M (1984) Samarium–neodymium data on two late Proterozoic ophiolites of Saudi Arabia and implications for crustal and mantle evolution. Contrib Mineral Petrol 85: 244–252

Dalziel IWD (1992) Late Precambrian rifted margins, the origin of the Iapetus and Pacific ocean basins, and Gondwana amalgamation: time and space considerations. EOS 73: 364

D'Amico C, Ibrahim HA, Sassi FP (1981) Outline of the Somalian Basement. Geol Rundsch 70: 882–896

Daniels JL (1965) Geology of the Borama and Hargeisa Districts, Somalia. Hargeisa. Geol Surv Som Rep: 118 pp

Debon F, Le Fort P (1983) A chemical–mineralogical classification of common plutonic rocks and associations. Trans R Soc Edinb Earth Sci 73: 135–149

DePaolo DJ (1981) Neodymium isotopes in the Colorado front range and crust–mantle evolution in the Proterozoic. Nature 291: 193–196

Didier J (1973) Granites and their Enclaves. Elsevier Scientific, Amsterdam, 393 pp

Doe BR, Zartman RE (1979) Plumbotectonics, the Phanerozoic. In: Barns HL (ed) Geochemistry of Hydrothermal Ore Deposits. Wiley Interscience, New York – Brisbane – Toronto, pp 22 – 70

Fabre J (1988) Les séries Paléozoïque d'Afrique: une approche. J Afr Earth Sci 7/1: 1 – 40

Gass IG (1977) The evolution of the Pan-African crystalline basement in NE Africa and Arabia. J Geol Soc London 134: 129 – 138

Gass IG, Ries AC, Shackleton RM, Smewing JD (1990) Tectonics, geochronology and geochemistry of the precambrian rocks of Oman. In: Robertson AHF, Searle MP, Ries AC (eds) The Geology and Tectonics of the Oman Region. Spec Publ Geol Soc London 49: 585 – 599

Govindaraju K (1984) Compilation of working values for 170 international reference samples of mainly silicate rocks and minerals. Geostandards Newsl Spec Issue, App I, Nancy, 8: 1 – 28

Gray CM, Oversby VM (1972) The behaviour of lead isotopes during granulite facies metamorphism. Geochim Cosmochim Acta 36: 939 – 952

Greenwood JE (1960) Report on the geology of the Las Koreh – Elayu area, Erigavo district, quarter degree sheets Nos. 5 and 6. Somaliland Protectorate Geol Surv 3: 36 pp

Greenwood JE (1961) The Inda Ad series of the former Somaliland Protectorate. Bull Overseas Geol Min Res, Oxford 8: 288 – 296

Greenwood WR, Anderson RE, Fleck RJ, Roberts RJ (1980) Precambrian geologic history and plate tectonics evolution of the Arabian shield. Bull Saudi Arabian Dir Gen Min Res 24

Haider A (1989) Géologie de la formation ferrifère Précambrienne et du complexe granulitique encaissant de Buur (Sud de la Somalie) – implications sur l'evolution crustale du socle de Buur. Unpubl PhD Thesis, Inst Nat Polytech de Lorraine, Nancy, 160 pp

Harms U, Schandelmeier H, Darbyshire DPF (1990) Pan-African reworked early/middle Proterozoic crust in NE Africa west of the Nile: Sr and Nd isotope evidence. J Geol Soc London 147; 859 – 872

Harris NBW, Duyverman HJ, Almond DC (1983) The trace element and isotope geochemistry of the Sabaloka igneous complex, Sudan. J Geol Soc London 140: 245 – 256

Harris NBW, Hawkesworth CJ, Ries AC (1984) Crustal evolution in northeast and east Africa from model Nd ages. Nature 309: 773 – 776

Harris NBW, Gass IG, Hawkesworth CJ (1990) A geochemical approach to allochthonous terranes: a Pan-African case study. Phil Trans R Soc London A 331: 533 – 548

Kennedy WQ (1964) The structural differentiation of Africa in the Pan-African (± 500 My) tectonic episode. Univ of Leeds, Res Inst African Geol, Dept Earth Sci, Ann Rep 8: 48 – 49

Key RH, Charsley TJ, Hackman BD, Wilkinson AF, Rundle CC (1989) Superimposed Upper Proterozoic collision-controlled orogenies in the Mozambique Belt of Kenya. Precambrian Res 44: 197 – 225

Klerkx J, Deutsch S (1977) Résultats préliminaires obtenus par la méthode Rb – Sr sur l'âge des formations précambriennes de la région d'Uweinat (Lybie). Mus Roy Afr Centr, Dept Geol Min, Ann Rep (1976): 83 – 94

Krogh TR (1973) A low contamination method for hydrothermal decomposition of zircon and extraction of U and Pb for isotopic age determination. Geochim Cosmochim Acta 37: 485 – 494

Kröner A (1977) Precambrian mobile belts of southern and eastern Africa – ancient sutures or sites of ensialic mobility? A case for crustal evolution towards plate tectonics. Tectonophysics 40: 101 – 135

Kröner A, Eyal M, Eyal Y, Sassi F, Teklay M (1989) Extensions of the Arabian – Nubian shield into southern Israel, Ethiopia and northern Somalia. Terra Abstr. EUG, Strasbourg, 1:363

Küster D (1990) Rare-metal pegmatites of Wamba, central Nigeria – their formation in relationship to late Pan-African granites. Miner Depos 25: 25 – 33

Küster D. Rb – Sr isotope systematics of muscovite from Pan-African pegmatites of western and northeastern Africa. Mineral Petrol, in press

Küster D, Harms U (1991) Late Proterozoic/Early Phanerozoic Rapakivi Granitoids in NE-Africa: evidence for Pan-African crustal consolidation. Abstr Vol, Int Symp Rapakivi Granites and Related Rocks, Helsinki, Finland, p 31

Küster D, Utke A, Leupolt L, Lenoir JL, Haider A (1990a) Pan-African granitoid magmatism in northeastern and southern Somalia. Berl Geowiss Abh, Berlin 120: 519 – 536

Küster D, Matheis G, Jacob KH, Mohamed FH, Caen-Vachette M (1990b) Geochemical indications of Pan-African rare-metal potentials in NE-Africa – variations in time and style. Berl Geowiss Abh, Berlin 120: 551 – 570

Lameyre J, Bowden P (1982) Plutonic rock types series – discrimination of various granitoid series and related rocks. J Volc Geotherm Res 14: 169 – 186

Lancelot JR (1975) Les systèmes U – Pb chronomètres et traceurs de l'évolution des roches terrestres. Unpubl PhD Thesis, Univ Paris VII, 280 pp

Lenoir JL, Haider A (1990) Contribution to the knowledge of the petrogenesis and geochronology of the Basement Complex of southern Somalia (Buur region). CIFEG Occasional Publ, 15th Coll African Geology, p 269

Ludwig KR (1980) Calculation of uncertainties of U – Pb isotope date. Earth Planet Sci Lett 46: 212 – 220

Mason JE, Warden AJ (1956) The Heis – Mait – Waqderia area. Somaliland Protectorate Geol Surv Rep 1: 23 pp

Merla G, Abbate E, Canuti P, Sagri M, Tacconi P (1973) Geological map of Ethiopia and Somalia, scale 1:2.000.000. Consiglio Nazionale delle Ricerche, Italy

Moorbath S, Welke HJ, Gale NH (1969) The significance of lead isotope studies in ancient, high-grade metamorphic basement complexes, as exemplified by the Lewisian rocks of northwest Scotland. Earth Planet Sci Lett 6: 245 – 256

Mosley PN (1993) Geological evolution of the late Proterozoic "Mozambique belt" of Kenya. Tectonophysics 221: 223 – 250

Muhongo S, Lenoir JL (1994) Pan-African granulite-facies metamorphism in the Mozambique belt of Tanzania: evidence from U – Pb on zircon geochronology. J Geol Soc London 151: 343 – 347

Pearce JA, Harris NBW, Tindle AG (1984) Trace element discrimination diagrams for the tectonic interpretation of granitic rocks. J Petrol 25/4: 956 – 983

Pinna P, Jourde G, Calvez JY, Mroz JP, Marques, JM (1993) The Mozambique Belt in northern Mozambique: Neoproterozoic (1100 – 850 Ma) crustal growth and tectogenesis, and superimposed Pan-African (800 – 550 Ma) tectonism. Precambrian Res 62: 1 – 59

Sacchi R, Zanferrari A (1987) Notes on some shear zones of northern Somalia. J Afr Earth Sci 6/3: 323 – 326

Shackleton RM (1986) Precambrian collision tectonics in Africa. In: Coward MP, Ries AC (eds) Collision Tectonics. Spec Publ Geol Soc London 19: 329 – 349

Snelling NJ (1963) Age determination unit. Ann Rep Overseas Geol Surv 1962, London, pp 30 – 39

Stacey JS, Kramers JD (1975) Approximation of terrestrial lead isotope evolution by a two-stage model. Earth Planet Sci Lett 26: 207 – 221

Stacey JS, Stoeser DB (1983) Distribution of oceanic and continental leads in the Arabian – Nubian Shield. Contrib Mineral Petrol 84: 91 – 105

Stacey JS, Doe BR, Roberts RJ, Delevaux MH, Gramlich JW (1980) A lead isotope study of mineralization in the Saudi Arabian Shield. Contrib Mineral Petrol 74: 175 – 188

Steiger RH, Jäger E (1977) Subcommission on geochronology: convention on the use of decay constants in geo- and cosmochronology. Earth Planet Sci Lett 36: 359 – 362

Stern RJ (1981) Petrogenesis and tectonic setting of Late Precambrian ensimatic volcanic rocks, Central Eastern Desert of Egypt. Precambrian Res 16: 195 – 230

Stoeser DB, Camp VE (1985) Pan-African microplate accretion of the Arabian Shield. Geol Soc Am Bull 96: 817–826

Taylor SR, McLennan SM (1981) The composition and evolution of the continental crust: rare earth element evidence from sedimentary rocks. Phil Trans R Soc London 301: 381–399

Utke A, Huth A, Matheis G, Hawa HH (1990) Geological and structural setting of the Maydh and Inda Ad basement units in northeast Somalia. Berl Geowiss Abh, Berlin 120: 537–550

Vidal P, Cocherie A, Le Fort P (1982) Geochemical investigations of the origin of the Manaslu leucogranite (Himalaya, Nepal). Geochim Cosmochim Acta 46: 2279–2292

Warden AJ (1981) Correlation and evolution of the Precambrian of the Horn of Africa and southwestern Arabia. Unpubl PhD Thesis, Mont-Univ, Leoben, 333 pp

Warden AJ, Horkel AD (1984) The geological evolution of the NE-branch of the Mozambique Belt (Kenya, Somalia, Ethiopia). Mitt Österr Geol Ges 77: 161–184

Whalen JB, Currie KL, Chappell BW (1987) A-type granites: geochemical characteristics, discrimination and petrogenesis. Contrib Mineral Petrol 95: 407–419

Williamson JH (1968) Least squares fitting of a straight line. Can J Phys 46: 1845–1847

Worku H, Yifa K (1992) The tectonic evolution of the Precambrian metamorphic rocks of the Adola Belt (southern Ethiopia). J Afr Earth Sci 14: 37–55

Zartman RE, Doe BR (1981) Plumbotectonics – the model. Tectonophysics 75: 135–162